Paper No.
08332

NACE INTERNATIONAL CORROSION 2008 CONFERENCE & EXPO

ROLES OF PASSIVATION AND GALVANIC EFFECTS IN LOCALIZED CO_2 CORROSION OF MILD STEEL

Jiabin Han, Yang Yang, Srdjan Nesic and Bruce N Brown
Institute for Corrosion and Multiphase Technology,
Department of Chemical and Biomolecular Engineering,
Ohio University
342 West State Street,
Athens, Ohio 45701

ABSTRACT

A galvanic mechanism of localized CO_2 corrosion was explored to explain a "mesa" type of localized CO_2 corrosion. Localized corrosion of mild steel in a deaerated environment dominated by CO_2 can be caused by local defects in the corrosion product film/scale covered surface. After the film is locally damaged, the bare surface, usually small in relation to the film covered surrounding area, corrodes one or more orders of magnitude faster than the film protected area. It was found that the open circuit potential (OCP) of the two surfaces is different, a higher OCP at the film covered surface (cathode) and a lower OCP at the bared surface (anode). The OCP difference between the anode and cathode drives the localized corrosion. The causes for this OCP difference between these surfaces were investigated. Studies using potentiodynamic sweeps have shown the passivation of the carbon steel surface, which was developed at higher pH under the $FeCO_3$ film. Cyclic polarization experiments reconfirmed the passivation phenomenon. The nature of the passivation was further explored by a depassivation experiment. The passive film dissolution or depassivation may help detach $FeCO_3$ film from substrate steel bulk and cause it to be removed more easily. These results have been combined into a 2-D galvanic mechanism, which can be used to explain the "mesa" localized CO_2 corrosion for mild steel.

Key Words: Localized CO_2 corrosion, galvanic mechanism, mesa attack, potentiodynamic, cyclic polarization, self-passivation, depassivation, passivation

INTRODUCTION

Severe localized CO_2 corrosion can be initiated due to a local damage to a protective $FeCO_3$ corrosion product film. The key questions related to the localized corrosion propagation can be summarized as follows:

- Why is the localized corrosion rate much higher than the uniform corrosion rate on bare metal surfaces under the same uniform bulk conditions?
- What is the driving force for the localized corrosion propagation?
- Under what conditions does the localized corrosion propagate?

A simple galvanic mechanism for localized CO_2 [1] corrosion propagation on mild steel has been already proposed, as summarized in Figure 1. Therefore some answers to the questions posed above are already known:

- Galvanic effect: The potential of the cathode (film covered surface) is more positive than that of the anode (pit area or bare steel surface). As a result, the anodic iron dissolution reaction can be accelerated one or more orders of magnitude at the small anode which is being polarized by the large cathode.
- "Grey zone" criterion: Localized corrosion propagates steadily when the solution is near saturation point with respect to $FeCO_3$.

There are still many open questions related to this localized corrosion mechanism that cannot be adequately explained, particularly pertaining to the reasons behind the potential difference between the film covered area (cathode) and the film-free area (anode). These were further investigated and are presented in the text below.

EXPERIMENTAL

Several tests were conducted in order to elucidate the details of the localized corrosion mechanism: potentiodynamic sweep, cyclic polarization (or cyclic voltammetry), self-passivation and depassivation tests. The first three test methods were used to investigate the passivation of mild steel in CO_2 aqueous electrolytes, which was suspected to have an impact on the localized corrosion. Passivation was observed after an external anodic potential was applied to the steel coupon and the detailed information will be discussed in the sections describing the potentiodynamic sweep and cyclic polarization tests. As spontaneous passivation was also observed in the absence of any external polarization, this is covered in the section on self-passivation tests. In depassivation tests, passive film breakdown was studied in such a way as to elucidate the link between passivation and localized corrosion.

Experimental Setup

The three electrode electrochemical cell depicted in Figure 2 was used for potentiodynamic sweep, cyclic polarization, self-passivation and depassivation tests. A rotating cylinder electrode (RCE) machined from a C1018 steel bulk was used as the working electrode (WE). A platinum ring, as a counter electrode (CE), was used in sweep, self-passivation and depassivation tests. A saturated Ag/AgCl reference electrode (SSE) was connected to the cell *via* a Luggin capillary through a porous Vycor frit. The electrochemical tests were done using a potentiostat. The temperature of the electrolytes was controlled automatically within ±1° of the preset value. Other conditions varied from test to test and are specified in the text below.

Procedures

In all tests, a 1 wt% NaCl (salt) aqueous electrolyte was deaerated by purging with a purified CO_2 for over 3 hours and the pH adjusted with sodium bicarbonate or hydrochloride acid. Prior to being immersed in the electrolyte, the steel coupons were prepared by polishing sequentially with 200, 400 and 600 grit sandpaper. They were then rinsed with isopropanol, ultrasonically cleaned and dried. The solution pH and ferrous iron concentration were continuously monitored during the tests. Open circuit potential (OCP) and polarization resistance were frequently measured. The anodic and cathodic Tafel slopes, 40mV and 120mV respectively, were used to calculate the corrosion rate from the polarization resistance. The potentiodynamic sweeps were started from the OCP at a scan rate of 0.2mV/s. Cathodical polarization was always executed first, in those experiments where both anodic and cathodic polarizations were done on the same specimen. In the cyclic polarization experiments the potential sweep was always started from the initial OCP in the positive direction and then reversed back to initial OCP at different rates: 0.2mV/s, 1mV/s and 5mV/s. In the self-passivation experiments the coupon was exposed to the corrosion environment without any external electrochemical stimuli. Once self-passivation was achieved, hydrochloric acid was added in order to decrease pH and cause depassivation.

Test Matrix

The test matrices for polarization tests are listed in Table 1 and Table 2. The self-passivation test conditions are summarized in Table 3. The depassivation process was investigated by decreasing pH after the self-passivation process was completed, and conditions are shown in Table 4.

RESULTS AND DISCUSSION

What Causes the Galvanic Effect in Localized CO_2 Corrosion of Mild Steel?

The open circuit potential increases after the protective ferrous carbonate film is formed, a phenomenon which was observed and reported in a previous publication [1]. However, based on the classic electrochemical kinetics theory, the OCP for the film covered surface should either be constant for a case when anodic and cathodic reactions are both retarded proportionally to the area coverage by the film (see Figure 3), or decrease as the cathodic reaction is more retarded due to the film also acting as a diffusion barrier for the cathodic species (see Figure 4). On the other hand, from the experimental observations, it is seen that the OCP (E_{corr}^{film}) increases as the corrosion rate decreases in the film forming experiments. This suggests that the anodic reaction is retarded more than the cathodic reaction what is typical for a steel passivation process. It is here assumed that the passivation is achieved due to the change in local electrolyte condition at the steel surface beneath the $FeCO_3$ film.

Passivation was Observed in Potentiodynamic Sweep Tests

The potential dynamic sweeps at a scan rate of 0.2mV/s were carried out from the OCP of an actively corroding steel surface, for different pH values varying from 4 to 8 (Figure 5). Steel passivation was observed only at pH 7 and 8 indicating that the passivation is more likely to occur under at high pH. Consistently with this conclusion, the passivation current and potential are higher at pH 7 than at pH 8.

In other words, passivation is possible only when the local pH is high enough, which can be true beneath a protective $FeCO_3$ film. While true surface pH is hard to measure (efforts are under way), one can calculate it readily. A case is depicted in Figure 6 using a simulation package MULTICORP V4 beta [(1)], showing clearly that the pH value near the steel surface can be much higher than that in the bulk. From the above information, it can be reasonably hypothesized that the local electrolyte condition beneath the $FeCO_3$ film may lead to the passivation of the steel surface. As a consequence, the corrosion rate can decrease to a much lower magnitude while at the same time its potential will increase to a more positive value. This qualitatively explains the measured open circuit potential drift in the positive direction during the film formation processes which has been previously reported [1].

Passivation was Observed in Cyclic Polarization Tests

In order to further investigate the nature of mild steel passivation, cyclic polarizations were carried out in deaerated NaOH solutions purged by N_2 as well as in $NaHCO_3$ solutions saturated by CO_2. Figure 7 shows the cyclic polarization curves for mild steel in the $NaHCO_3$ solution at pH 8 using different scan rates: 0.2 mV/s, 1mV/s and 5mV/s. Passivation is seen in those cases where the current density decreases as the potential increases. Comparing the cyclic polarization curves at three scan rates, a lower passivation current density and potential are observed at a lower scan rate, i.e. when the passive film is given more time to form. The cyclic polarization curves for mild steel in N_2 purged NaOH solution at different scan rates are shown in Figure 8. Mild passivation is observed only at the lowest scan rate 0.2mV/s. This suggests that passivation is more difficult to obtain in the absence of CO_2, and that the $FeCO_3$ which forms in CO_2 aqueous solution assists the passivation.

Spontaneous Passivation Observations

Clearly the passivation of mild steel in CO_2 solutions can be achieved by anodic polarization, i.e. by accelerating the anodic reaction. Therefore, a new series of experiments was done to establish if this will also happen spontaneously, at the OCP. This is termed “self-passivation” and will be discussed in the following sections.

Self-passivation under a simulated local environment beneath a $FeCO_3$ film was observed at bulk pH values from 7.1 to 8.1. The self-passivation tests (see Figure 9) show that the time to reach self-passivation is longer at lower pH levels.

The self-passivation curves are shown in Figure 10 for tests at different temperatures at the same pH 7.8. The time to reach self-passivation is longer at lower temperatures, as expected since decreasing the temperature slows down the process kinetics.

Data collected under 80°C and pH 8 at different ratios of partial pressures of CO_2 demonstrated in Figure 11 show that self-passivation could be achieved even with only 0.07 bar CO_2. In contrast, no self-passivation was observed in deaerated pure NaOH solution during the period of the test. The data (see Figure 12) obtained under pure deaerated NaOH solution by purging N_2 at pH 9.5 show that no self-passivation could be achieved even at such a high pH. Even when the steel coupon was subjected to a $6A/m^2$ anodic current density, which corresponds to a corrosion rate as 2-3 times than that in CO_2

(1) MULTICORP is a corrosion software package developed by the Institute for Corrosion and Multiphase Technology at Ohio University.

solution under the same conditions, no significant passivation was observed at pH 8 in deaerated NaOH solution (Figure 13). This clearly reiterates that the passivation is not only a function of pH and that CO_2 is directly involved in the passivation process of mild steel.

As a summary of passivation investigations, it was clearly demonstrated that passivation of mild steel can be achieved under $FeCO_3$ films in CO_2 corrosion. This contributes to the OCP increase during the film formation process and results in the potential difference between bare steel surface and the passivated film covered area, which is the origin of the galvanic effect (shown in Figure 14).

What Causes Passivation beneath a $FeCO_3$ Film?

To better understand passivation and what causes it, depassivation tests were conducted. Data for some of the tests are shown in Figure 15, Figure 16 and Figure 17. Self-passivation is achieved after 60 hours. If Figure 15 and Figure 16 are examined carefully, it can be observed that the depassivation process occurred in the range from pH 7.8 to pH 5.4.

Is $FeCO_3$ Exclusively Responsible for Passivation and Depassivation?

The hypothesis can be postulated that passivation is caused by the $FeCO_3$ formation and that depassivation is initiated if this film is lost due to a decrease in pH. This seems to be a plausible explanation for the self-passivation and depassivation observations. Figure 17 shows a passivation/depassivation plot for "Case 1", with sections labeled with pH and values for $FeCO_3$ supersaturation (calculated from the model by W. Sun, *et al* [2]) which governs $FeCO_3$ formation. Note that the solution conditions with respect to $FeCO_3$ remain supersaturated (supersaturation (SS) >>1) as the pH was decreased and the passivation was gradually lost. This implies that the ferrous carbonate film did not dissolve, and in spite of that the carbon steel depassivated. The survival of iron carbonate films was confirmed by scanning electron microscopy. Similar phenomenon can be seen in "Case 2" (Figure 18). According to the hypothesis, depassivation and repassivation should happen around supersaturation of 1 what was not the case. Unstable depassivation is found at much higher supersaturation (SS=8−23).

These observations lead us to ***reject*** the hypothesis that the precipitation/dissolution of ferrous carbonate is solely responsible for passivation/depassivation of mild steel in CO_2 solutions. The question then arises: what is the alternative explanation?

Does $Fe(OH)_2$ Formation and Dissolution Cause the Passivation and Depassivation?

Based upon thermodynamic calculations [3], it can be shown that ferrous hydroxide is stable in the near-neutral pH conditions used in the tests. Therefore the new hypothesis can be: the steel is passivated when the ferrous hydroxide film is formed; depassivation occurs when solution conditions are undersaturated with respect to $Fe(OH)_2$. Figure 19 and Figure 20 show the same data as in Figure 17 and Figure 18, respectively, but with the passivation/depassivation regions labeled with $Fe(OH)_2$ supersaturation values. Figure 19 shows that passivation is obtained when solution conditions are supersaturated with respect to ferrous hydroxide (based on the valid data at 25 °C [4]). Conversely, depassivation is observed when conditions are undersaturated. The unstable depassivation region in Figure 20 is observed when ferrous hydroxide is near its solubility limit whilst ferrous carbonate is still

supersaturated. "Case 3", depicted in Figure 21, supports the above hypothesis. However, passivation was not observed in a system without CO_2 which implies that the formation of iron carbonate may be essential in this case. While, this is clearly a plausible scenario, it has not been established beyond reasonable doubt that it is exactly ferrous hydroxide that is responsible for passivation, there is a suite of similar compounds that need to be considered before any firm conclusions are drawn. It is expected that ongoing surface analysis will offer complementary evidence.

A GALVANIC MECHANISM AND THE "MESA" CORROSION OF MILD STEEL

Incorporation of the information presented above into the previously formulated galvanic corrosion mechanism for localized attack on steel in CO_2 solutions allows us to more accurately predict the sequence of events in the evolution of the so called "mesa corrosion", as shown in Figure 22. This is a typical form of localized corrosion seen in the oil and gas upstream industry. The mechanism can be summarized as follows: In the initial stage (Figure 22, 8-1), the steel is exposed to a corrosive environment. A ferrous carbonate film can form when its solubility limit is exceeded (Figure 22, 8-2). This causes an increase in the local pH beneath the ferrous carbonate film. Consequently a ferrous hydroxide passive film can be formed, resulting in the potential increase (Figure 22, 8-3). Localized corrosion may be initiated when the ferrous carbonate film is locally damaged due to mechanical or chemical effects (Figure 22, 8-4). The ferrous hydroxide is then exposed to the bulk environment where the pH is lower. As a result, the ferrous hydroxide film dissolves and the steel is locally depassivated, leading to the exposure of its bare surface to bulk solution conditions (Figure 22, 8-5). The potential of the large surrounding surface covered by passive ferrous hydroxide film and protective ferrous carbonate film is higher than that of the bare metal surface. This results in the bare steel patch corroding at a very high rate due to the galvanic effect (Figure 22, 8-6). This is accompanied by corrosion and passive film dissolution in the lateral direction (Figure 22, 8-7). Detachment of the iron carbonate film occurs. The removal of the detached film causes the pit to grow wider (Figure 22, 8-8).

CONCLUSIONS

- Passivation of mild steel in CO_2 solutions has been observed in cyclic polarization and potentiodynamic sweep tests. The self-passivation is also found to occur and is affected by pH, temperature and CO_2 concentration.
- It has been preliminarily hypothesized that $Fe(OH)_2$ forms under the $FeCO_3$ film and is responsible for the steel passivation process. Conversely, the depassivation is caused by the dissolution of the passive film which can occur once the protective iron carbonate film is lost due to mechanical or chemical attack.
- Passivation results in a significant open circuit potential increase of mild steel. This may lead to establishment of a galvanic cell between the film covered passive area and the actively corroding bare steel surface. This scenario can be used to explain the sequence of event leading to mesa type localized corrosion.

REFERENCES

1. J. Han, Y. Yang, B. Brown, S. Nesic, "Electrochemical Investigation of Localized CO2 Corrosion on Mild Steel". Corrosion/2007, paper No. 07323, (Houston, TX: NACE, 2007).
2. W. Sun, PhD dissertation. Ohio University, 2006.
3. M. Pourbaix, "Atlas of Electrochemical Equilibria in Aqueous", (English Edition), Oxford: Pergamon Press, 1966, pp. 307-321.
4. D. R. Lide, "CRC Handbook of Chemistry and Physics", 85th edition, Boca Raton, CRC Press LLC, 2005.

Table 1 Potentiodynamic sweep test matrix

Coupon material	C1018 RCE
Coupon area /cm^2	5-5.3
Temperature /°C	80
Partial pressure of CO_2 /bar	0.52
pH	4-8
Solution	1wt% NaCl
Initial Fe^{2+} concentration /ppm	0
Flow	stagnant
Polarization speed /(mV/s)	0.2
Anodic polarization range /(V vs. OCP)	0.2, 0.3
Cathodic polarization range /(V vs. OCP)	-0.2

Table 2 Cyclic polarization test matrix

Material	C1018 RCE
Solution	1wt% NaCl
pH adjusted by	NaOH, $NaHCO_3$
Temperature /°C	80
N_2 partial pressure /bar	0, 0.52
CO_2 partial pressure /bar	0, 0.52
pH	8
Cyclic voltammetry scan rate /mV/s	0.2, 1, 5
Polarization range (vs. OCP) /mV	0 to 500

Table 3 Test matrix for self-passivation tests

Material	C1018 RCE
Solution	1wt% NaCl
pH adjusted by	NaOH, $NaHCO_3$
Temperature /°C	80
N_2 partial pressure /bar	0.52, 0.45
CO_2 partial pressure /bar	0, 0.07, 0.52
pH	8, 9.5
Galvanostatic current density /A/m^2	0, 6

Table 4 Test matrix for depassivation test

Coupon material	C1018
Coupon area / cm^2	5.2
Temperature / °C	80
Partial pressure of CO_2 / bar	0.53
pH for self-passivation	7.8
Salt concentration / wt%	1
Solution stirring	stagnant
pH decrease	7.8→5.5

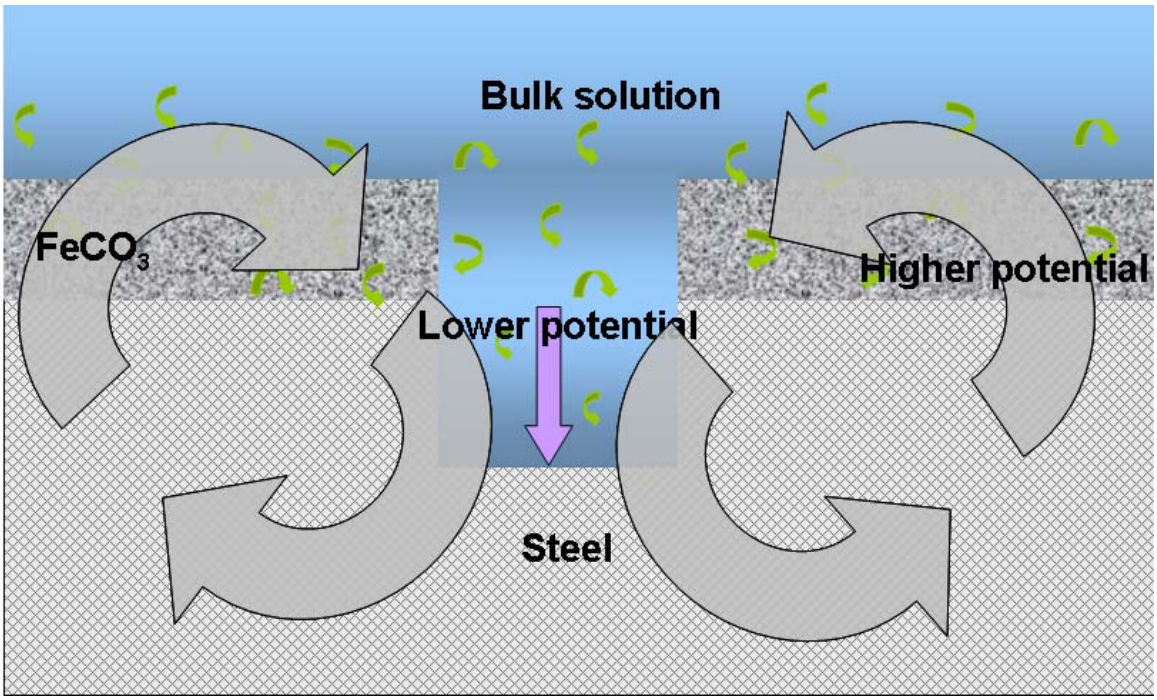

Figure 1 1-D galvanic mechanistic model for localized CO_2 corrosion on mild steel

Figure 2 Sketch of three electrode cell used in tests [2]

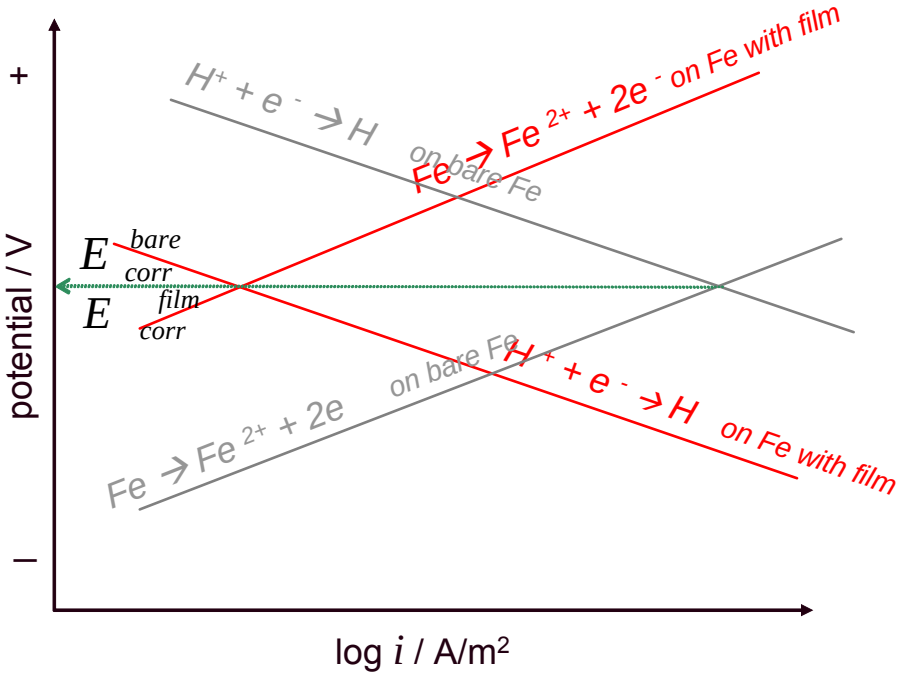

Figure 3 Open circuit potential keep constant for filmed and bare surface where both anodic and cathodic reactions are reduced proportional to area covering effect

[2] The sketch is taken from universal facility picture at Institute for Corrosion and Multiphase Technology.

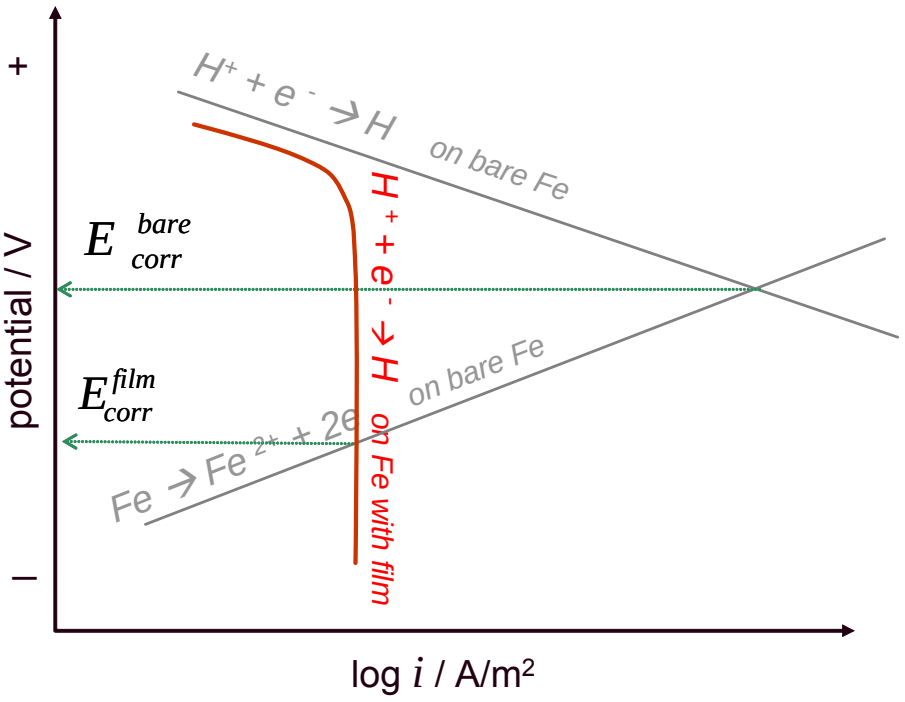

Figure 4 Open circuit potential decreases for film covered surface where cathodic reaction is mass transfer controlling due to diffusion barrier.

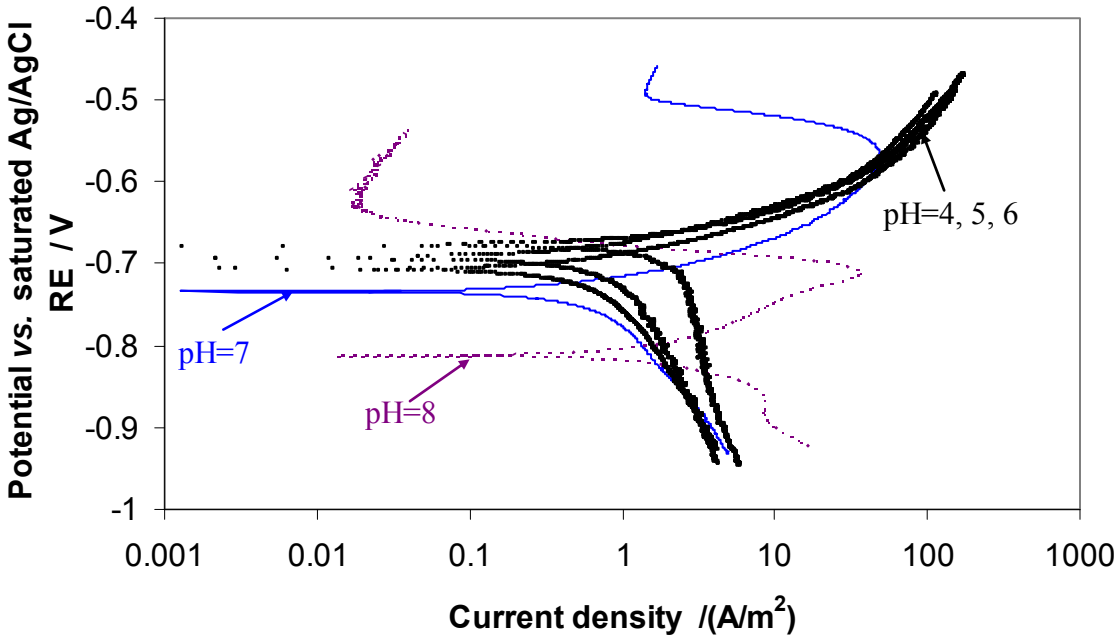

Figure 5 Sweep curves on active surfaces at [NaCl] =1%wt, T=80°C, pCO_2=0.53 bar, stagnant solution

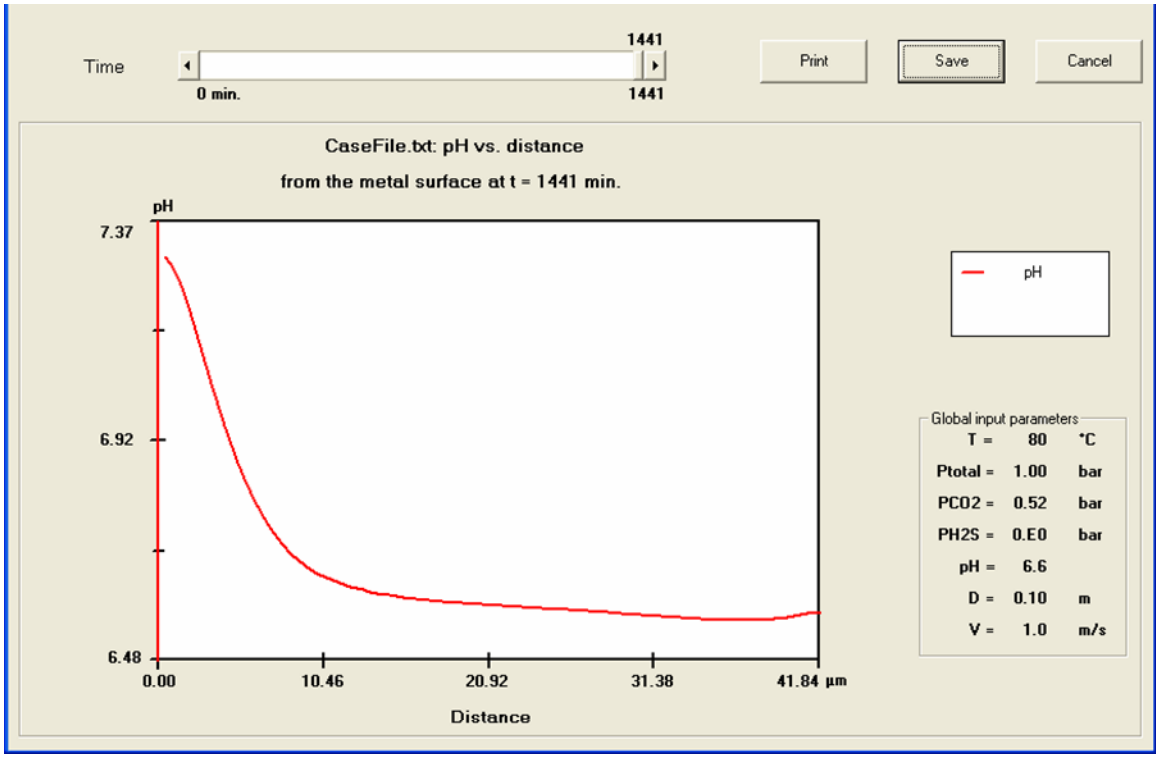

Figure 6 A case simulation for pH change vs. distance to metal surface after a protective $FeCO_3$ film was formed

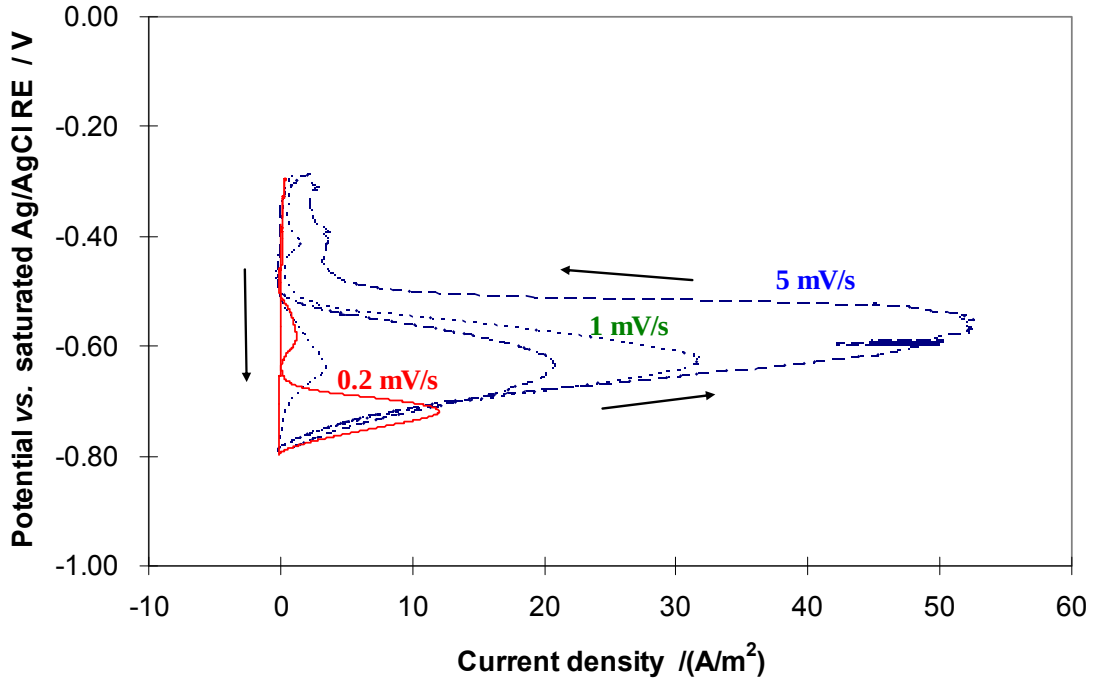

Figure 7 Cyclic polarization curve of mild steel at different scan rate in CO_2 purged $NaHCO_3$ solution under T=80°C, pH=8.

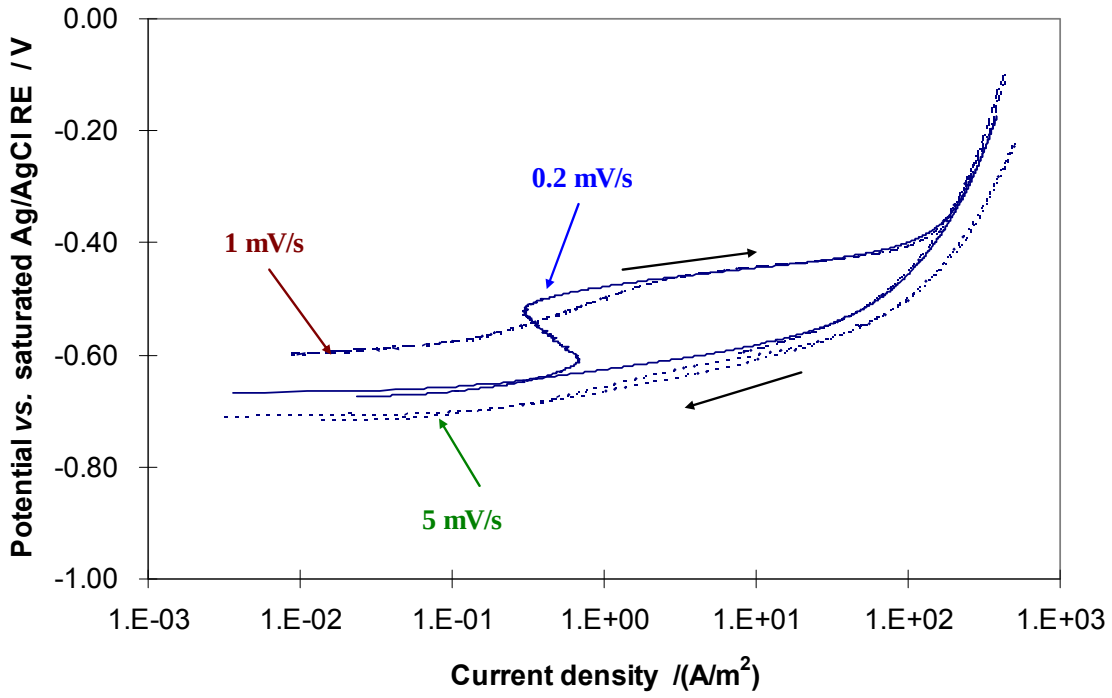

Figure 8 Cyclic polarization curve of mild steel at different polarization rate in deaerated NaOH solution under T=80°C, pH8.

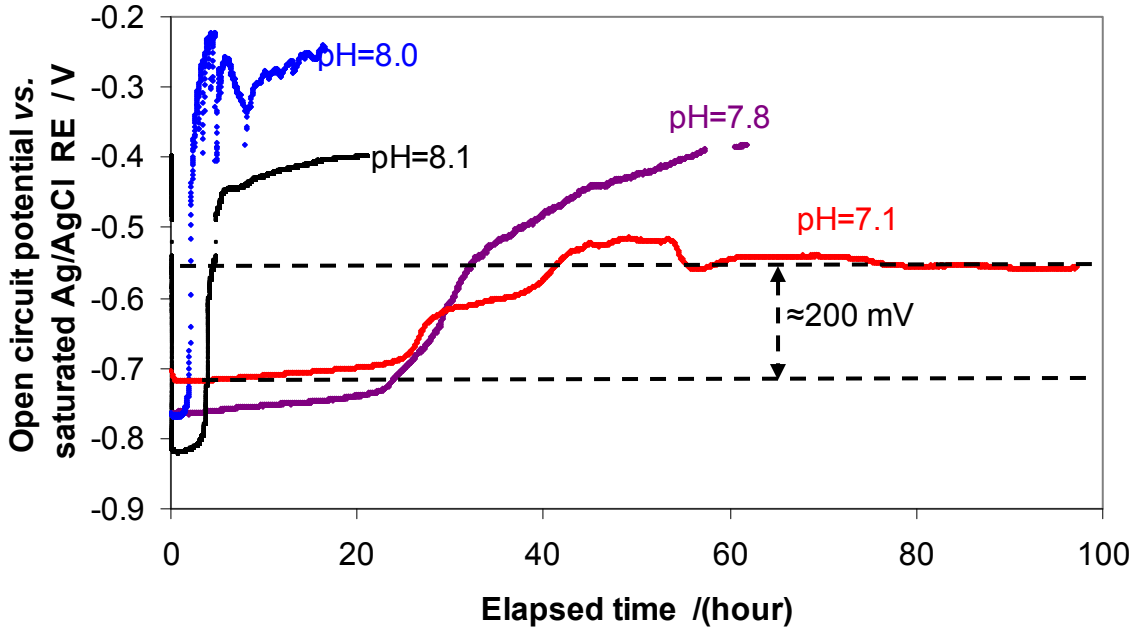

Figure 9 The self-passivation is affected by pH at T=80°C, P_{CO2}=0.53 bar, [NaCl] =1%wt, stagnant solution

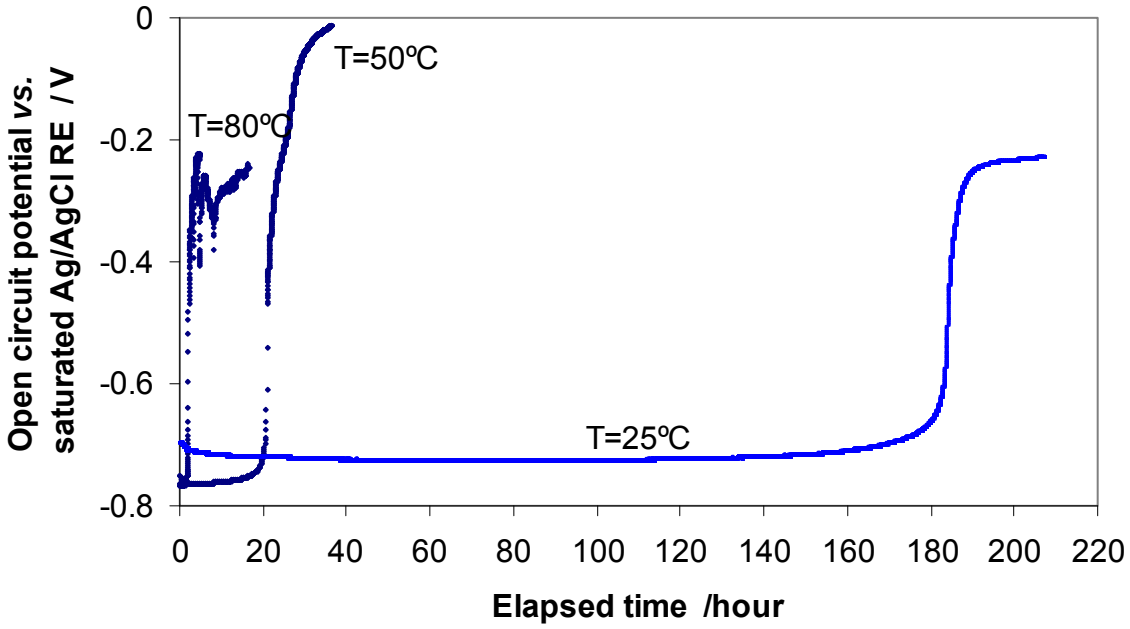

Figure 10 The self-passivation is affected by temperature at pH=7.5, P_{CO2}=0.53 bar, [NaCl] =1%wt, stagnant solution

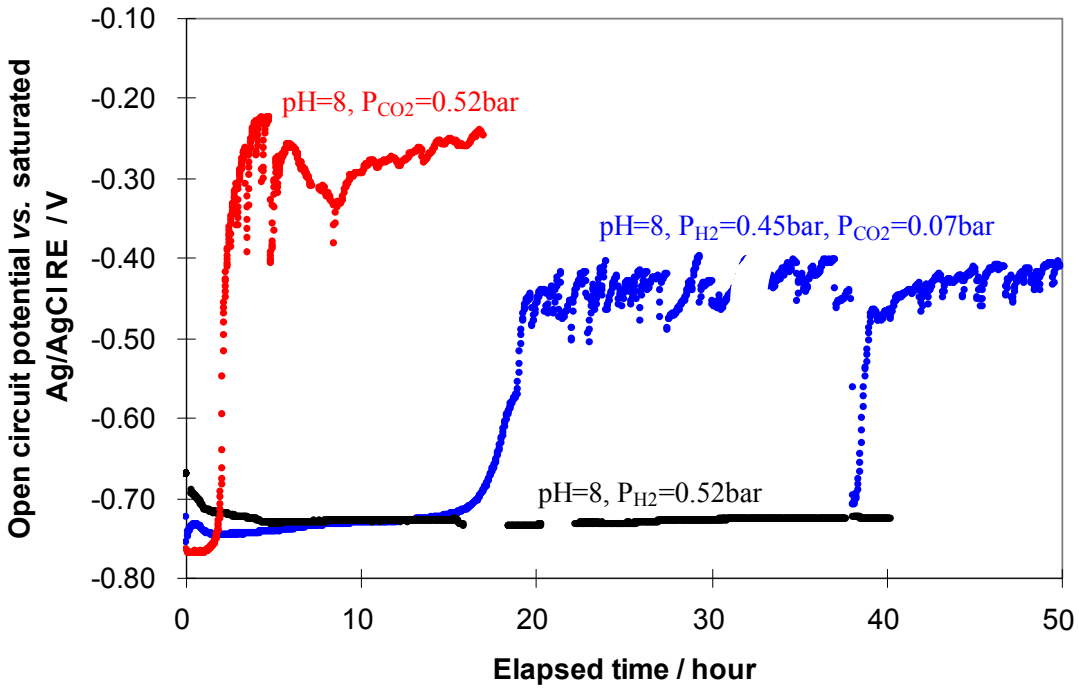

Figure 11 Open circuit potential vs. time of mild steel in NaOH system under T=80°C, pH8, P_{N2}=0.45 bar, P_{CO2}=0.07 bar.

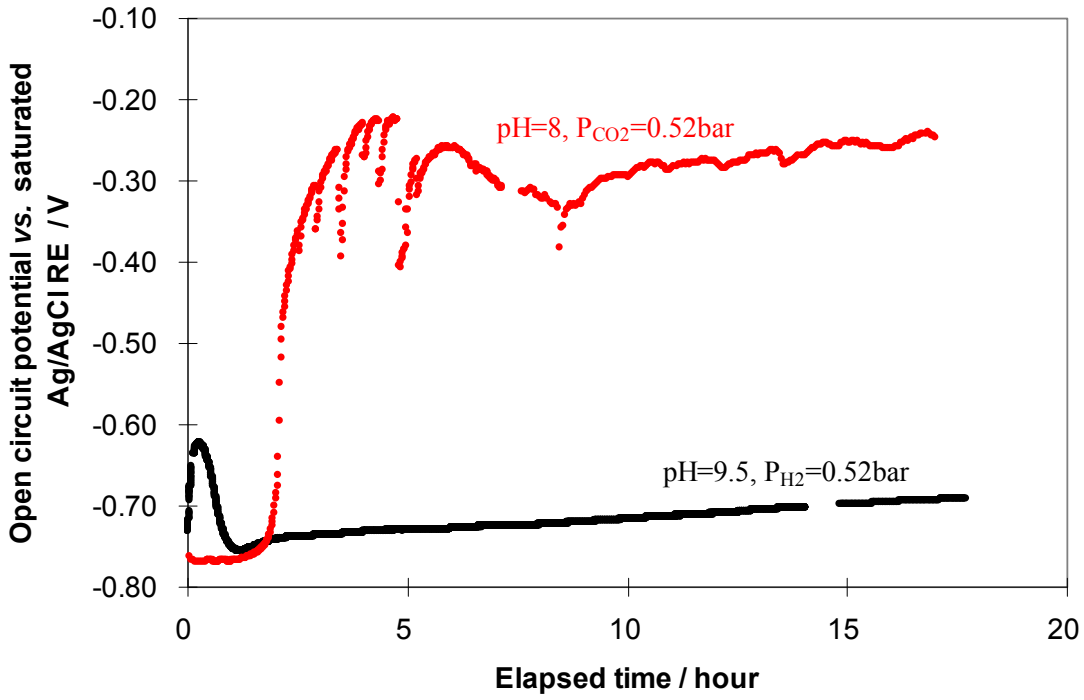

Figure 12 Open circuit potential vs. time of mild steel in NaOH system at pH9.5, P_{N2}=0.52 bar

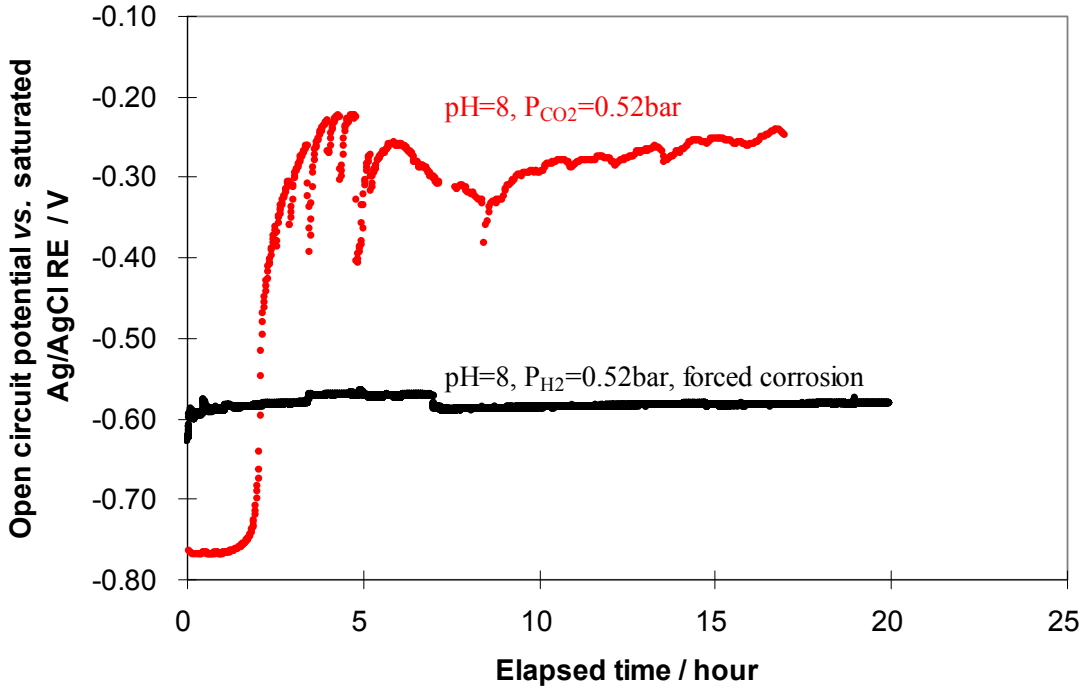

Figure 13 Open circuit potential vs. time of mild steel in NaOH system at pH8, P_{N2}=0.52 bar, anodic current=6 A/m^2

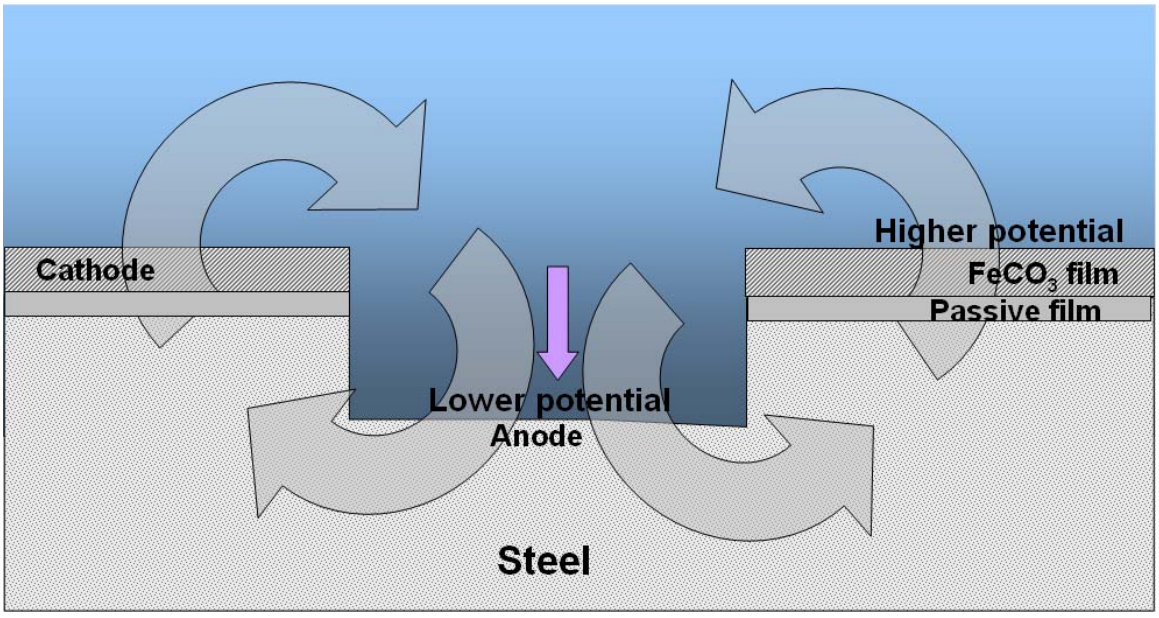

Figure 14 A galvanic effect of localized corrosion is due to the passivation under local condition beneath the $FeCO_3$ film

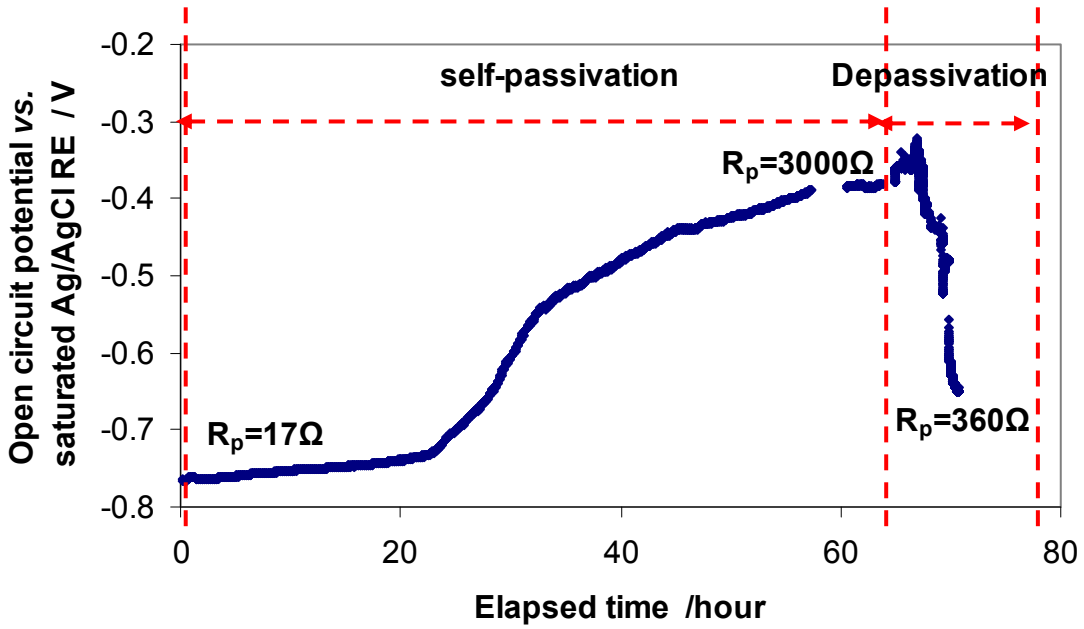

Figure 15 Case1: The self-passivation (at initial pH=7.8, T=80°C, P_{CO2}=0.53 bar, [NaCl] =1%wt, stagnant solution) and depassivation by decreasing pH from pH 7.8 to pH 5.4 (case 1)

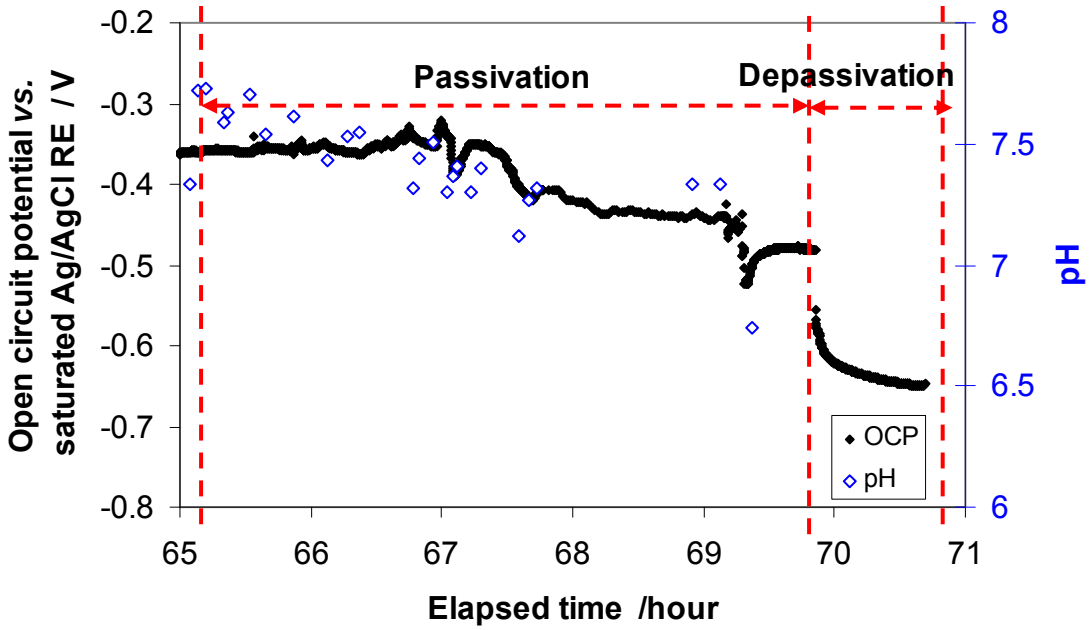

Figure 16 Case1: The depassivation process by decreasing pH at initial pH=7.8, T=80°C, P_{CO2}=0.53 bar, [NaCl] =1%wt, stagnant solution. Solid diamonds represent the pH (case 1)

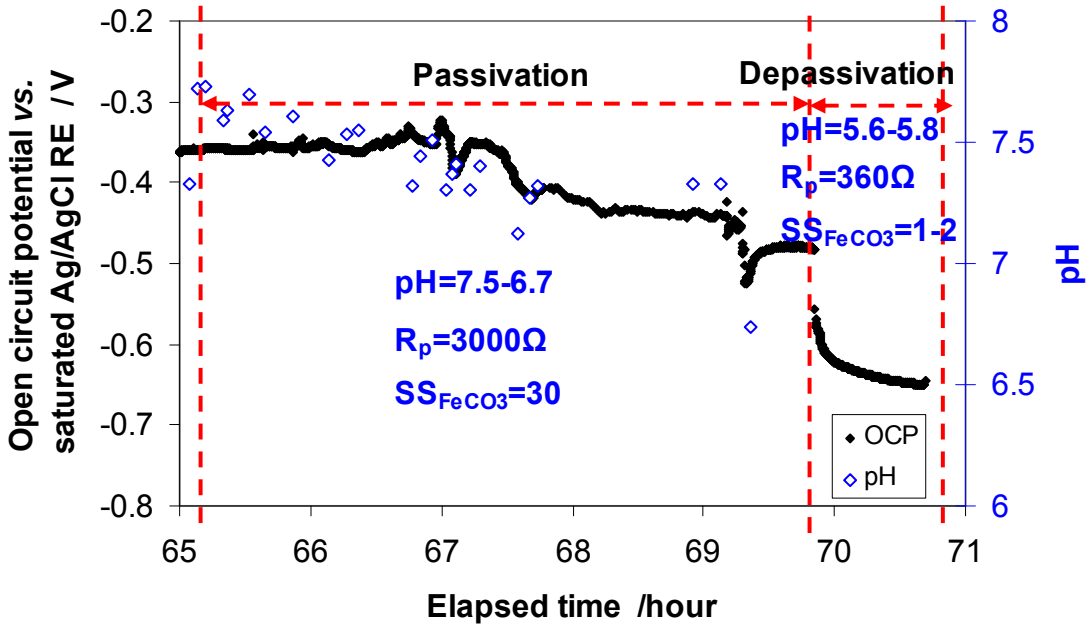

Figure 17 Case 1: relation between supersaturation of $FeCO_3$ and depassivation at T=80°C, P_{CO2}=0.53 bar, [NaCl] =1%wt, mild stirred

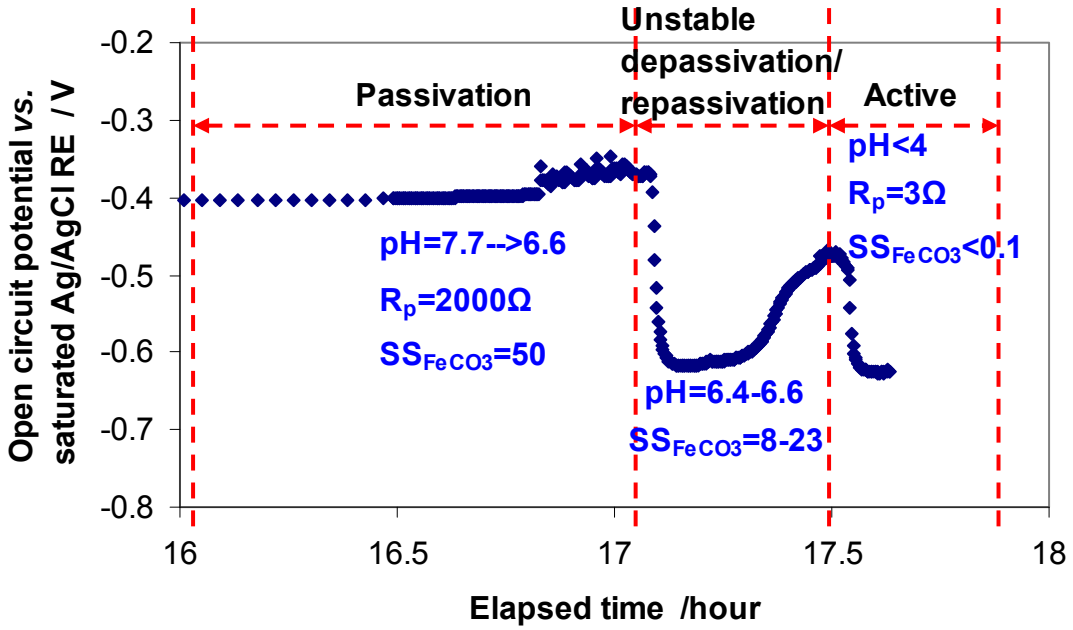

Figure 18 Case 2: relation between supersaturation of $FeCO_3$ and unstable depassivated or re-passivation at T=80°C, P_{CO2}=0.53 bar, [NaCl] =1%wt, mild stirred

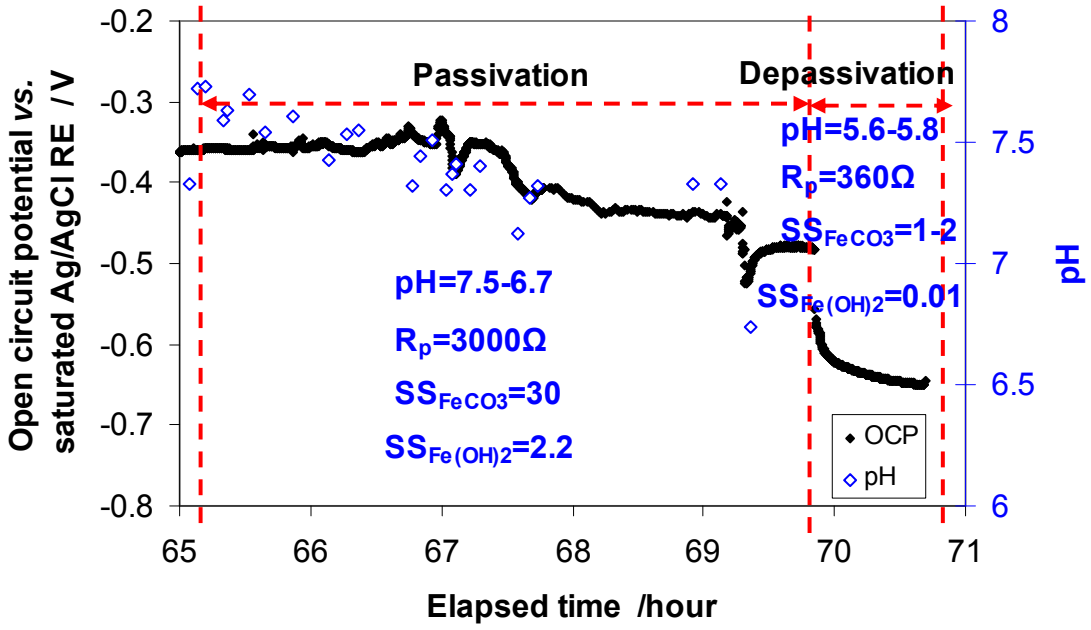

Figure 19 Case 1: relation between supersaturation of $FeCO_3$ or $Fe(OH)_2$ and depassivation at T=80°C, P_{CO2}=0.53 bar, [NaCl] =1%wt, mild stirred

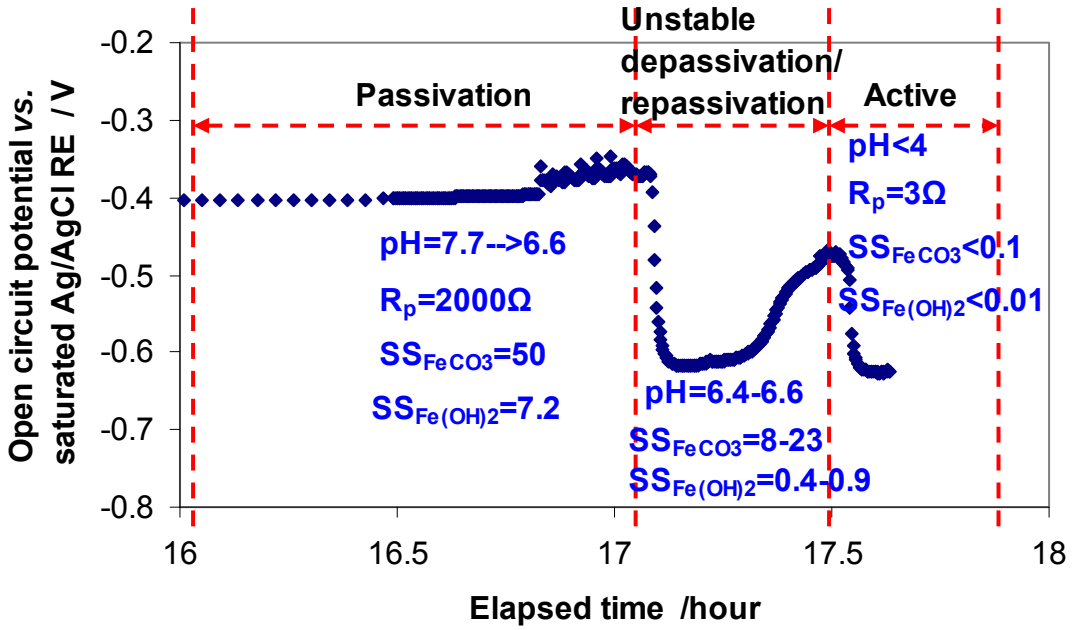

Figure 20 Case2: relation between supersaturation of $FeCO_3$ or $Fe(OH)_2$ and unstable depassivation at T=80°C, P_{CO2}=0.53 bar, [NaCl] =1%wt, mild stirred flow

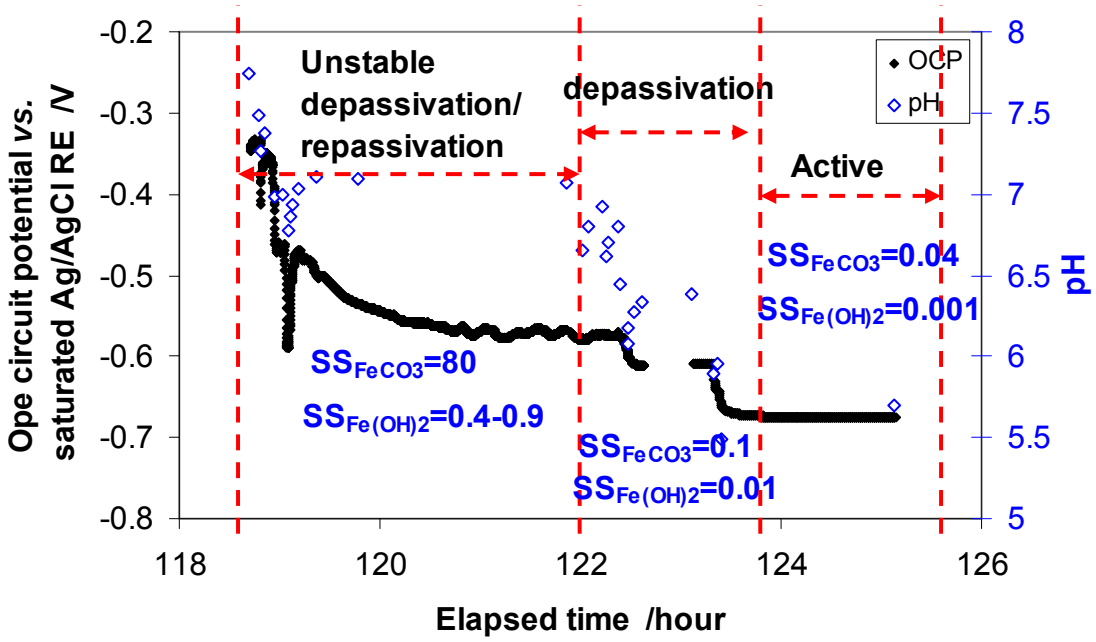

Figure 21 Case3: relation between supersaturation of $FeCO_3$ or $Fe(OH)_2$ and unstable depassivation or depassivation at T=80°C, P_{CO2}=0.53 bar, [NaCl] =1%wt, mild stirred flow

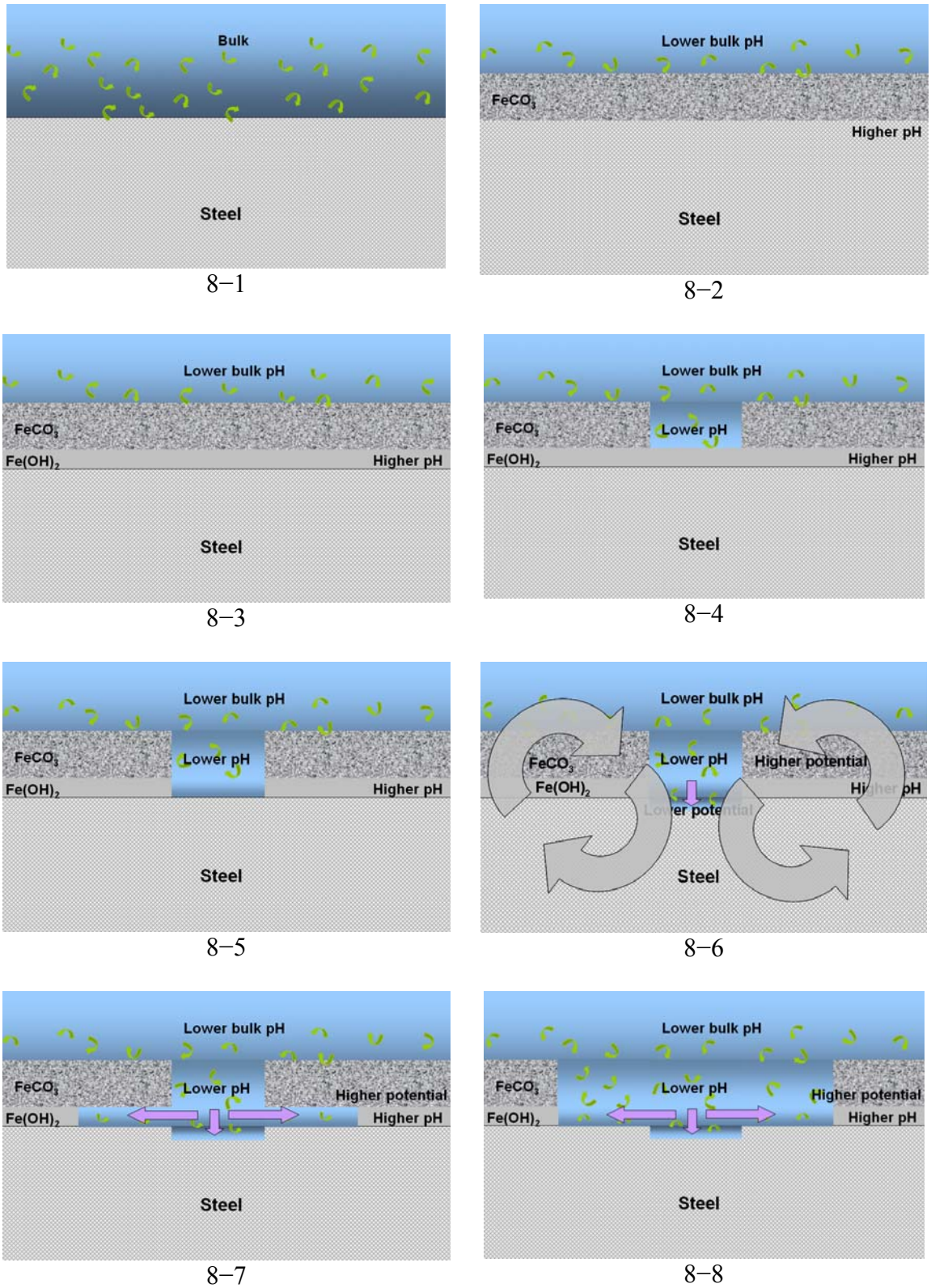

Figure 22 The 2-D mechanism for "mesa" type localized CO_2 corrosion on mild steel